

A minimum ductility design method for non-rectangular high-strength concrete beams

F. T. K. Au[†] and A. K. H. Kwan[‡]

*Department of Civil Engineering, The University of Hong Kong, Hong Kong
(Received May 19, 2003, Revised January 15, 2004, Accepted February 2, 2004)*

Abstract. The flexural ductility of solid rectangular reinforced concrete beams has been studied quite extensively. However, many reinforced concrete beams are neither solid nor rectangular; examples include T-, Γ -, Π - and box-shaped beams. There have been few studies on the flexural ductility of non-rectangular reinforced concrete beams and as a result little is known about the possible effect of sectional shape on flexural ductility. Herein, the effect of sectional shape on the post-peak flexural behaviour of reinforced normal and high-strength concrete beams has been studied using a newly developed analysis method that employs the actual stress-strain curves of the constitutive materials and takes into account the stress-path dependence of the stress-strain curve of the steel reinforcement. It was revealed that the sectional shape could have significant effect on the flexural ductility of a concrete beam and that the flexural ductility of a T-, Γ -, Π - or box-shaped beam is generally lower than that of a solid rectangular beam with the same overall dimensions and the same amount of reinforcement provided. Based on the numerical results obtained, a simple method of ensuring the provision of a certain minimum level of flexural ductility to non-rectangular concrete beams has been developed.

Keywords: flexural ductility; high-strength concrete; reinforced concrete beams.

1. Introduction

The simplest sectional shape of a reinforced concrete beam is a solid rectangular section. A solid rectangular concrete beam requires only simple formwork for casting and usually has good all round structural performance in terms of not just flexural strength, but also shear strength, torsional rigidity, lateral stability and robustness. However, the structural efficiency of a solid rectangular concrete beam is relatively low, especially when the beam design is governed by flexural strength. This is because when the beam is subjected to flexural loading, the concrete near the neutral axis contributes little to flexural strength. That is why for a long span beam, in which case the flexural strength requirement is most critical, a non-rectangular sectional shape, such as T-, Γ -, Π - or box, is usually adopted. As most of the concrete is located at the extreme compressive end rather than near the neutral axis of the beam section, a T-, Γ -, Π - or box-shaped beam is in general structurally more efficient than a solid rectangular beam.

It should nevertheless be noted that such optimisation of the sectional shape of a concrete beam for maximum flexural strength could lead to lower performance in the other structural aspects such as shear strength, torsional rigidity, lateral stability and robustness. More care is generally needed in

[†] Associate Professor

[‡] Professor and Associate Dean

the design of a non-rectangular concrete beam. However, there is one particular structural aspect that has often been overlooked: flexural ductility. A non-rectangular concrete beam might have a similar flexural strength compared to that of a solid rectangular concrete beam with the same overall dimensions and the same amount of steel reinforcement provided, but it could also have a significantly lower flexural ductility. Whether the lower flexural ductility of the non-rectangular concrete beam would cause any structural safety problem requires careful checking, but it seems that most engineers are ignoring this, probably due to the numerical difficulties involved in the evaluation of the flexural ductility of a non-rectangular concrete beam.

Although it is well known that both strength and ductility are important for structural safety and that in the flexural design of a reinforced concrete beam it is necessary to provide a certain minimum level of flexural ductility to avoid brittle failure, relatively little attention has been paid to the flexural ductility design of reinforced concrete beams. It was only until recent years when high-strength concrete, which is generally more brittle than normal concrete, gradually became more commonly used that some engineers started to pay more attention to the flexural ductility of reinforced concrete beams, especially those made of high-strength concrete (Carreira and Chu 1986, Skeikh and Yeh 1992, Samra, *et al.* 1996, Pam, *et al.* 2001a). However, the evaluation of the flexural ductility of a concrete beam is rather difficult. Whilst the flexural strength of a concrete beam can be determined quite easily using the ordinary beam bending theory, it is not possible to evaluate the flexural ductility using any simple method. To evaluate the flexural ductility of a concrete beam, a complete moment-curvature analysis extended well into the post-peak range is needed. Such kind of analysis is highly nonlinear and involves stress-path dependence of the constitutive materials during strain reversal at the post-peak stage (Pam, *et al.* 2001b, Ho, *et al.* 2003). The complexities involved may help to explain why flexural ductility analysis is seldom carried out and most engineers choose to ignore the problem.

The author's research team has recently developed a new method of moment-curvature analysis that takes into account the actual stress-strain curves and stress-path dependence of the constitutive materials and can be applied to analysis at the post-peak stage to produce the complete moment-curvature curve for ductility evaluation (Pam, *et al.* 2001b, Ho, *et al.* 2003). Using this newly developed method of analysis, the effects of various structural parameters including the concrete grade, the compression and tension steel yield strengths and the compression and tension steel area ratios on the flexural ductility of reinforced concrete beams have been quite thoroughly studied (Pam, *et al.* 2001b, Ho, *et al.* 2003, Kwan, *et al.* 2004). Based on the numerical results obtained, new design methods for "concurrent flexural strength and ductility design" and "minimum ductility design" of reinforced high-strength concrete beams have been developed (Kwan, *et al.* 2002, Ho, *et al.* 2004). However, the previous studies have been limited to solid rectangular concrete beams and consequently the design methods developed based on these studies are applicable only to solid rectangular beams.

In the present study, the afore-mentioned analysis method has been expanded to cope with non-rectangular beam sections. Using the expanded analysis method, the nonlinear flexural behaviour and flexural ductility of T-, Γ -, Π - and box-shaped beams cast of normal or high-strength concrete have been analysed. By varying the shape parameters of the beam sections analysed, the effect of sectional shape on the flexural ductility of non-rectangular high-strength concrete beams has been studied and a minimum ductility design method for non-rectangular concrete beams developed.

2. Method of analysis

The constitutive model for unconfined concrete developed by Attard and Setunge (1996), which has been shown to be applicable to a broad range of concrete strength from 20 to 130 MPa, is adopted in the moment-curvature analysis. The stress-strain curve of the constitutive model is given by:

$$\sigma_c/f_{co} = \frac{K_1(\epsilon_c/\epsilon_{co}) + K_2(\epsilon_c/\epsilon_{co})^2}{1 + (K_1 - 2)(\epsilon_c/\epsilon_{co}) + (K_2 + 1)(\epsilon_c/\epsilon_{co})^2} \quad (1)$$

in which σ_c and ϵ_c are the compressive stress and strain at any point on the stress-strain curve, f_{co} and ϵ_{co} are the compressive stress and strain at the peak of the stress-strain curve, and K_1 and K_2 are coefficients dependent on the concrete grade. It should be noted that f_{co} is actually the in-situ uniaxial compressive strength, which may be estimated from the cylinder or cube compressive strength using appropriate conversion factors. Fig. 1(a) shows some typical stress-strain curves so derived.

For the steel reinforcement, a linearly elastic-perfectly plastic stress-strain curve is adopted. Since there could be strain reversal in the steel reinforcement at the post-peak stage despite monotonic increase of curvature (Pam, *et al.* 2001b, Ho, *et al.* 2003), the stress-strain curve of the steel is stress-path dependent. It is assumed that when strain reversal occurs, the unloading path of the stress-strain curve is linear and has the same slope as the initial elastic portion of the stress-strain curve. Fig. 1(b) shows the resulting stress-strain curve of the steel reinforcement.

Only three other basic assumptions have been made in the analysis: (1) plane sections before bending remain plane after bending, (2) the tensile strength of concrete is negligible, and (3) there is no bond-slip between concrete and steel. These assumptions are widely accepted in the literature (Park and Paulay 1975). The moment-curvature behaviour of the beam section is analysed by applying prescribed curvatures to the beam section incrementally starting from zero. At a prescribed curvature, the strain profile in the section is first evaluated based on the above assumptions. From the strain profile so obtained, the stresses developed in the constitutive materials are determined from their respective stress-strain curves. The stresses developed have to satisfy the axial

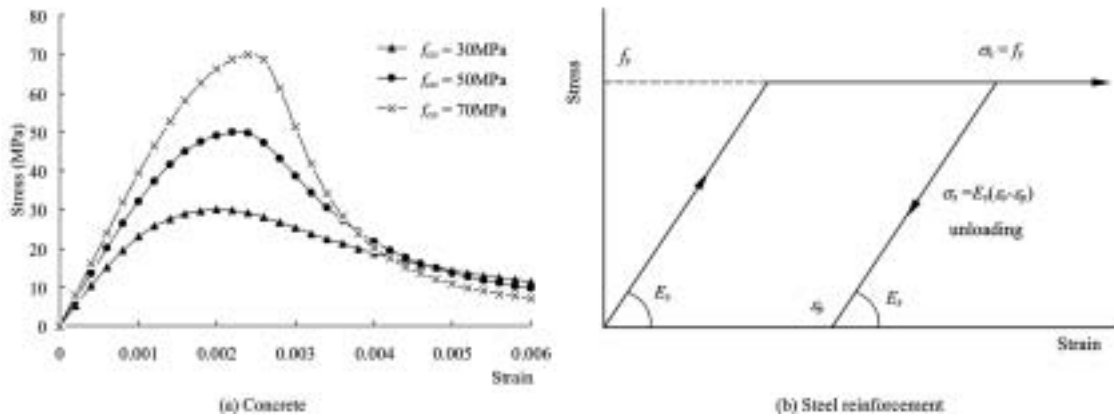


Fig. 1 Stress-strain curves of concrete and steel reinforcement

equilibrium condition, from which the neutral axis depth is evaluated by iteration. Having determined the neutral axis depth, the resisting moment is calculated from the moment equilibrium condition. The above procedure is repeated until the curvature is large enough for the resisting moment to increase to the peak and then decrease to lower than 50% of the peak moment.

The method of analysis applied to non-rectangular sections and that applied to solid rectangular sections are basically the same. T-, Γ -, Π - and box-shaped sections are analysed as equivalent T-shaped sections, as shown in Fig. 2. In the equivalent T-shaped section, the flange breadth B is taken as the total breadth of the section, the web breadth B_w is taken as the total breadth of the web(s), the flange depth D_f is taken as the depth of the flange subjected to compression, and the web depth D is taken as the effective depth of the section (the distance between the tension reinforcement and the extreme concrete compression fibre). The equivalent T-shaped section is provided with tension reinforcement of sectional area A_{st} and compression reinforcement of sectional area A_{sc} at depths of D and D_1 respectively below the extreme concrete compression fibre. It is noteworthy that L- and inverted T-shaped sections subjected to hogging moment may also be analysed as equivalent T-shaped sections subjected to sagging moment. The mathematical equations involved and the numerical techniques employed in the analysis are explained in the following. When the curvature of the beam section is increased to ϕ , the strain developed is given by:

$$\epsilon = \phi x \tag{2}$$

where x is the distance from the neutral axis. Therefore, the compressive strain ϵ_{ce} at the extreme concrete compression fibre, the compressive strain ϵ_{sc} in the compression reinforcement and the tensile strain ϵ_{st} in the tension reinforcement can be respectively written as:

$$\epsilon_{ce} = \phi d_n \tag{3a}$$

$$\epsilon_{sc} = \phi(d_n - D_1) \tag{3b}$$

$$\epsilon_{st} = \phi(D - d_n) \tag{3c}$$

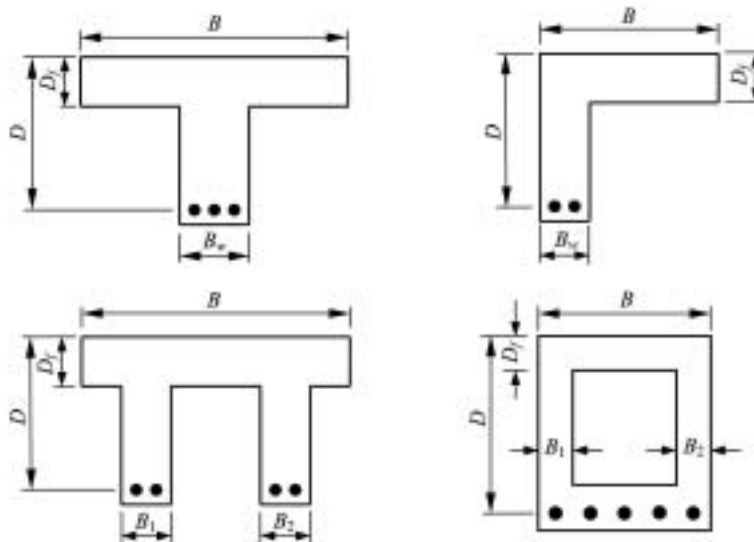


Fig. 2 Analysis of T-, Γ -, Π - and box-shaped sections

in which d_n is the neutral axis depth. The corresponding stresses σ_c , σ_{sc} and σ_{st} developed in the concrete, compression reinforcement and tension reinforcement can then be evaluated from the respective stress-strain curves of the materials.

The stresses developed in the beam section must satisfy the conditions of axial equilibrium and moment equilibrium. Axial equilibrium leads to

$$P = \int_0^{d_n} \sigma_c b dx + \sum A_{sc} \sigma_{sc} - \sum A_{st} \sigma_{st} \quad (4)$$

where P is the applied axial load (compressive force taken as positive) and b is the width of the section at x from the neutral axis. On the other hand, moment equilibrium leads to

$$M = \int_0^{d_n} \sigma_c b x dx + \sum A_{sc} \sigma_{sc} (d_n - D_1) + \sum A_{st} \sigma_{st} (D - d_n) \quad (5)$$

where M is the resisting moment (sagging moment taken as positive).

Because of the variable width of the non-rectangular beam section, a more sophisticated numerical integration technique has to be used when integrating over the concrete section to determine the axial force and the resisting moment contributed by the stresses developed in the concrete. In the present study, Romberg integration (Gerald and Wheatley 1999), which can significantly improve the accuracy of the simple trapezoidal rule when the integrand is known at equispaced intervals, has been adopted. The non-rectangular section is first divided into trapezoidal components, each having its width b varying as a linear function of the distance from neutral axis x . An initial estimate of the integral is obtained by the trapezoidal rule using equispaced intervals of h . By halving the interval h and reapplying the trapezoidal rule, one may then take advantage of the property that the error of integration is of the order of the second power of the interval, i.e., $O(h^2)$, to obtain a more accurate estimate of the integral. Assuming that the error $O(h^2)$ is proportional to h^2 (error $\approx C h^2$), a better estimate of the integral of $O(h^4)$ accuracy may be obtained by solving for the unknown constant C from the previous two estimates of the integral. This process can be continued by further halving the interval h until the desired accuracy is achieved.

The axial equilibrium condition as shown in Eq. (4) can be used to determine the neutral axis depth d_n . Normally, given a specified curvature ϕ and a trial value of neutral axis depth d_n , the equilibrium condition is not immediately satisfied and there is an unbalanced axial force R . Since the relation between the unbalanced axial force R and the neutral axis depth d_n is nonlinear, an iterative scheme is required to determine the value of d_n which will give a zero value of R . The scheme adopted here is the modified linear interpolation method (Gerald and Wheatley 1999). Before the iterations, an initial pair of trial values of d_n are chosen so that their values of unbalanced axial force R are of opposite sign. Let the neutral axis depth and the unbalanced axial force at the $(i-1)$ th iteration be d_n^{i-1} and R^{i-1} respectively and those at the (i) th iteration be d_n^i and R^i respectively. The value of d_n^{i+1} for the $(i+1)$ th iteration, which is expected to give a smaller unbalanced axial force, is evaluated as:

$$d_n^{i+1} = d_n^i - \frac{R^i}{R^i - R^{i-1}} (d_n^i - d_n^{i-1}) \quad (6)$$

Unless the unbalanced axial force R^{i+1} for the $(i+1)$ th iteration is sufficiently small, the pair of trial values of d_n have to be updated. One of the trial values of d_n with an unbalanced axial force R having the same sign as R^{i+1} will be replaced by d_n^{i+1} with the unbalanced axial force R^{i+1} . The other trial value will have the value of d_n retained but the unbalanced axial force R reduced by half, as illustrated in Fig. 3. The strategy of always using a pair of trial values of d_n with values of R of opposite sign to continue with the iteration so that the iteration proceeds by interpolation is to avoid infinite loops in computation around local minima/maxima. As opposed to the case of a rectangular section, the relation between the unbalanced force R and the neutral axis depth d_n for a non-rectangular section often has kinks around locations of abrupt change in breadth, leading to local minima/maxima. As extrapolation from trial points near a local minimum/maximum could lead to infinite looping, it is essential that the iteration scheme rely on interpolations rather than extrapolations. The strategy of halving the unbalanced force R of the retained trial value of d_n is to speed up the rate of convergence. Both strategies are suggested by Gerald and Wheatley (1999).

3. Flexural behaviour of non-rectangular sections

3.1. Sections analysed

For the sake of comparing the flexural behaviour of a non-rectangular beam section to that of a rectangular beam section with the same overall dimensions, two beam sections, one rectangular and one non-rectangular (a T-shaped section), have been analysed. The two beam sections analysed, shown in Fig. 4, have the same overall dimensions of $B = 1000$ mm and $D = 1500$ mm. For the T-shaped section, the web breadth and flange depth are given by $B_w = 400$ mm and $D_f = 300$ mm respectively. No compression reinforcement is provided. Two separate cases with different amounts of tension reinforcement provided have been considered. In Case 1, the amount of tension reinforcement A_{st} provided in each section is $30,000$ mm², while in Case 2, the amount of tension reinforcement A_{st} provided in each section is $75,000$ mm². For a preliminary study, the in-situ concrete compressive strength f_{co} is fixed at 50 MPa while the tension steel yield strength f_{yt} is fixed at 460 MPa. Regarding the Young's modulus of the steel reinforcement, it is assumed to have a constant value of $E_s = 200$ GPa.

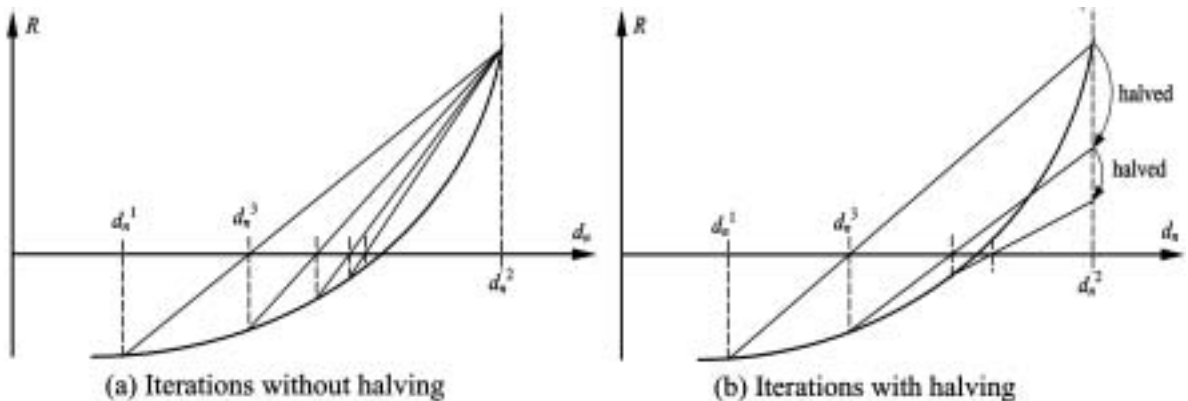


Fig. 3 Modified linear interpolation method

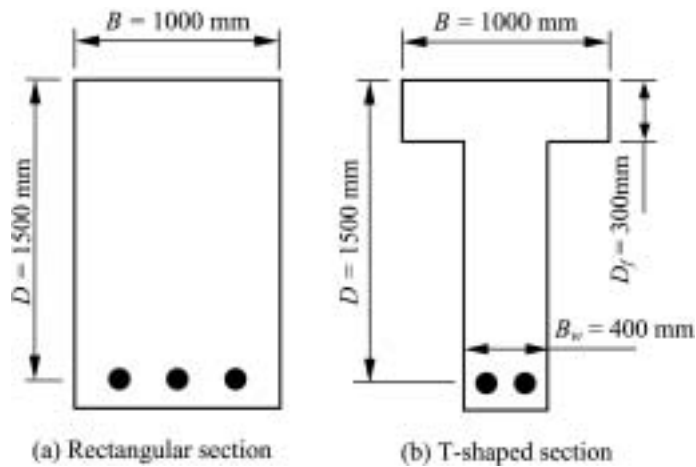


Fig. 4 Beam sections analysed

3.2. Complete moment-curvature curves

The complete moment-curvature curves obtained for Case 1 and Case 2 are shown in Fig. 5(a) and Fig. 5(b) respectively. In Case 1, it is seen that the rectangular section and the T-shaped section, each provided with the same amount of tension reinforcement, have similar peak resisting moments. They both fail in tension (i.e., the tension reinforcement yields before the concrete fails). Thus, both the rectangular section and the T-shaped section are under-reinforced. That is why both these two sections fail in a ductile manner, as evidenced by the presence of a flat yield plateau in each of their moment-curvature curves. Nevertheless, it is obvious that the flexural ductility of the T-shaped section is significantly lower than that of the rectangular section. On the other hand, in Case 2, the rectangular section and the T-shaped section, though each provided with the same amount of tension reinforcement, have somewhat different peak resisting moments. Relatively, the peak

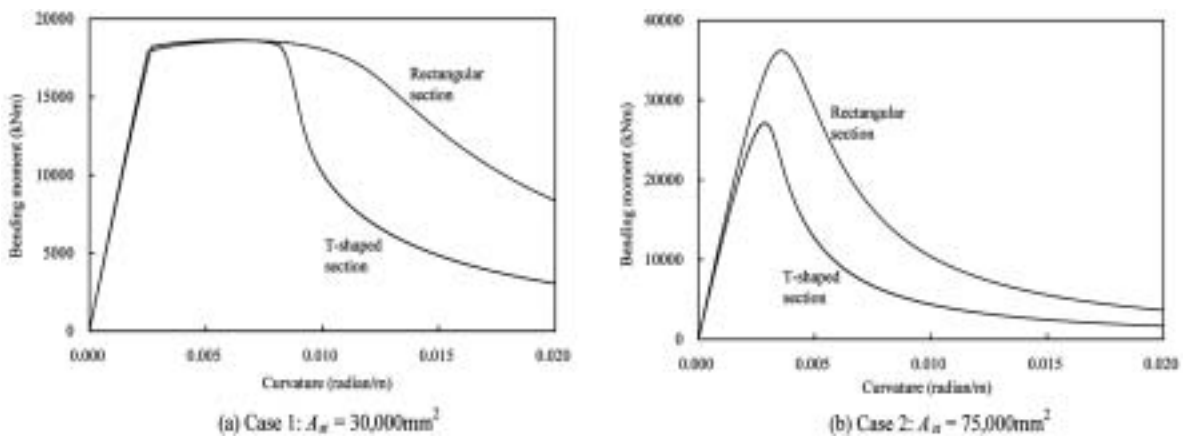


Fig. 5 Moment-curvature curves of beam sections analysed

resisting moment of the T-shaped section is lower than that of the rectangular section. They both fail in compression (i.e., the tension reinforcement remains unyielded even when the concrete has failed completely). Thus, both the rectangular section and the T-shaped section are over-reinforced. As a result, they both fail in a brittle manner, as evidenced by the absence of any yield plateau in their moment-curvature curves. Again, it appears that the flexural ductility of the T-shaped section is significantly lower than that of the rectangular section.

3.3. Neutral axis depth and strain in tension reinforcement

The variations of the neutral axis depth and the strain in the tension reinforcement with the applied curvature in Case 1 and Case 2 are shown in Fig. 6(a) and Fig. 6(b) respectively. In Case 1 (under-reinforced sections), the neutral axis depths of the rectangular section and the T-shaped section remain more or less constant until the two sections reach their respective peak resisting moments. When the two sections have reached their respective peak resisting moments, the neutral axis depths start to decrease. Then, in each section, at a certain point within the post-peak stage, the neutral axis depth starts to increase. In the T-shaped section, the neutral axis depth starts to increase at an earlier time and once it starts to increase it increases at a faster rate than in the rectangular section. Consequently, in the T-shaped section, the strain reversal of the tension reinforcement happens at an earlier time and once strain reversal happens the strain of the tension reinforcement drops more quickly than in the rectangular section. This explains why the T-shaped section has a significantly lower flexural ductility than that of the rectangular section. In Case 2 (over-reinforced sections), the neutral axis depths of the rectangular section and the T-shaped section remain more or less constant until the respective peak resisting moments are reached but thereafter start to increase. As before, the neutral axis depth of the T-shaped section starts to increase at an earlier time and once it starts to increase it increases at a faster rate than in the rectangular section. Because of this, in the T-shaped section, strain reversal of the tension reinforcement happens earlier and the strain of the tension reinforcement drops more quickly than in the rectangular section leading to a significantly lower flexural ductility of the T-shaped section compared to that of the rectangular section.

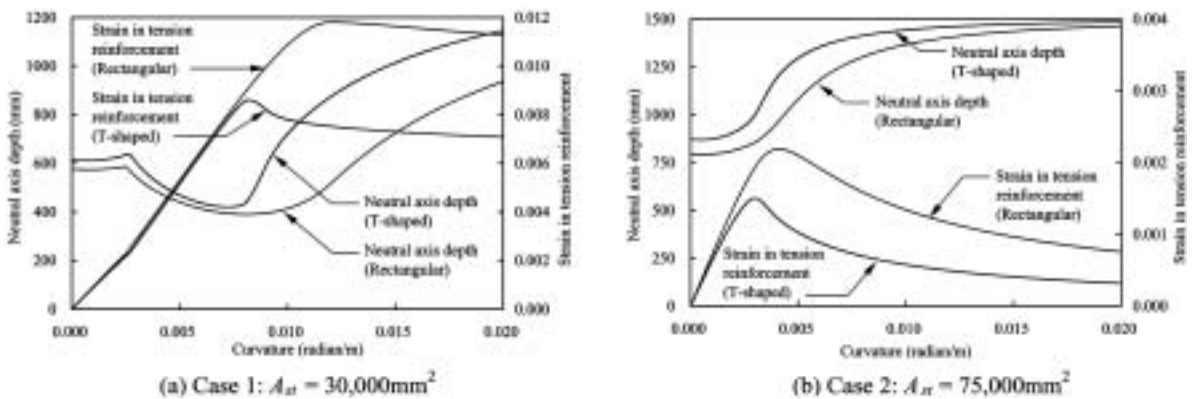


Fig. 6 Neutral axis depth and strain in tension reinforcement

4. Flexural ductility of non-rectangular sections

4.1. Flexural ductility evaluation

The flexural ductility of the beam section may be evaluated in terms of a curvature ductility factor μ defined by:

$$\mu = \phi_u / \phi_y \quad (7)$$

where ϕ_u and ϕ_y are the ultimate curvature and yield curvature respectively. The ultimate curvature ϕ_u is taken as the curvature of the beam section when the resisting moment of the beam section has, after reaching the peak value of M_p , dropped to $0.8 M_p$. On the other hand, the yield curvature ϕ_y is taken as the curvature at the hypothetical yield point of an equivalent linearly elastic-perfectly plastic system with an elastic stiffness equal to the secant stiffness of the section at $0.75 M_p$ and a yield moment equal to M_p .

4.2. Flexural ductility of rectangular and non-rectangular sections

When comparing the flexural ductility of a non-rectangular section to that of a rectangular section with the same overall dimensions, it is necessary to take into account also the other structural parameters such as the concrete grade and the amount of tension reinforcement provided because the flexural ductility varies significantly with these parameters. The two beam sections shown in Fig. 4 are reanalysed using different values of f_{co} and A_{st} . To study the effect of the concrete grade, f_{co} is set equal to 30, 50 or 70 MPa. To study the effect of the amount of tension reinforcement provided, A_{st} is varied from 15,000 to 75,000 mm². Fig. 7 shows the variation of the curvature ductility factor μ with the tension steel area A_{st} for the two beam sections analysed at different concrete grades.

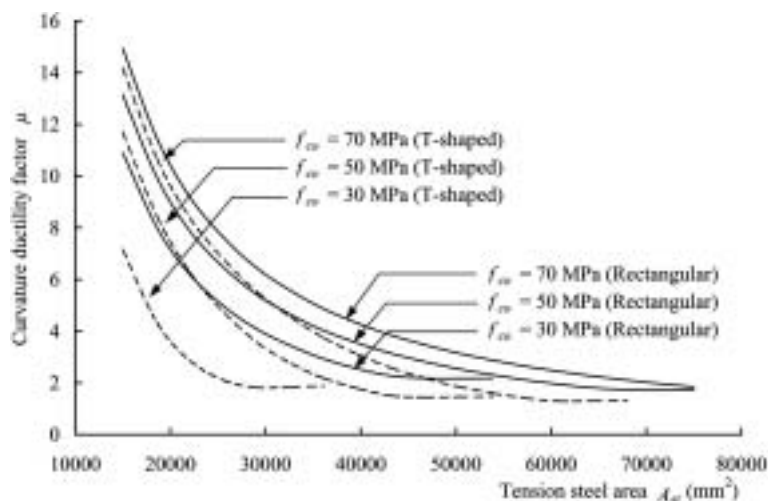


Fig. 7 Variation of curvature ductility factor μ with tension steel area A_{st}

It can be seen from the results for $f_{co} = 50$ MPa that the flexural ductility of a beam section, regardless of whether the section is rectangular or non-rectangular, decreases as the tension steel area increases. For the rectangular section, the value of μ decreases from 13.1 to 1.7 when the tension steel area increases from 15,000 mm² to 70,000 mm² and then remains at around 1.7 when the tension steel area further increases. For the T-shaped section, the value of μ decreases from 11.7 to 1.5 when the tension steel area increases from 15,000 mm² to 50,000 mm² and then remains at around 1.5 when the tension steel area further increases. In general, at the same concrete grade and the same tension steel area, the flexural ductility of a T-shaped section is lower than that of a rectangular section with the same overall dimensions.

It is also evident from the figure that the concrete grade has significant effect on the flexural ductility. In both the cases of rectangular and T-shaped sections, the flexural ductility increases slightly with the concrete grade, albeit a higher grade concrete should be less ductile. This is because when a higher grade concrete is used, the tension reinforcement tends to yield at an earlier time leading to a slightly longer yield plateau in the moment-curvature curve. This may also be explained by looking at the degree of the beam section being under- or over-reinforced. The balance steel area $A_{st,bo}$ is larger when the concrete grade is higher. Thus, relatively, at the same tension steel area A_{st} , the tension to balanced steel ratio (the ratio $A_{st}/A_{st,bo}$) is smaller when a higher grade concrete is used. The tension to balanced steel ratio may be interpreted as a measure of the degree of the beam section being under/over-reinforced. When the tension to balanced steel ratio is smaller, the degree of the beam section being under-reinforced is higher and the degree of the beam section being over-reinforced is lower. Therefore, at the same tension steel area, the degree of the beam section being under-reinforced increases with the concrete grade and as a result the flexural ductility increases slightly with the concrete grade.

4.3. Variation of flexural ductility with tension to balanced steel ratio

From the above, it is obvious that one major structural parameter determining the flexural ductility is the tension to balanced steel ratio, which is denoted hereafter by λ ($\lambda = A_{st}/A_{st,bo}$). Fig. 8 shows the variation of the curvature ductility factor μ with the tension to balanced steel ratio λ for the two beam sections analysed at different concrete grades. It is seen that regardless of the concrete grade and the shape of the beam section, μ decreases as λ increases and then remains roughly constant when $\lambda > 1.0$. At the same concrete grade and the same tension to balanced steel ratio, the μ -value of the T-shaped section is slightly higher than that of the rectangular section when $\lambda < 0.6$ (i.e., when the sections are lightly reinforced) and the μ -value of the T-shaped section is slightly lower than that of the rectangular section when $\lambda > 0.8$ (i.e., when the sections are heavily reinforced). Nevertheless, the difference in the μ -values of the rectangular and T-shaped sections at the same tension to balanced steel ratio is much smaller than the difference in the μ -values of the rectangular and T-shaped sections at the same tension steel area. Hence, it may be said that the single most important structural parameter determining the flexural ductility of a beam section is the tension to balanced steel ratio λ . Relatively, the change of sectional shape from rectangular to T-shape has only secondary effect on the flexural ductility; it affects the flexural ductility mainly by reducing the balanced steel area of the beam section and thus at a given tension steel area, a T-shaped section would have a higher tension to balanced steel ratio and a lower flexural ductility.

Fig. 8 also better reveals the effect of concrete grade on flexural ductility than Fig. 7. From Fig. 8, it can be seen that regardless of the shape of the beam section, at the same tension to balanced

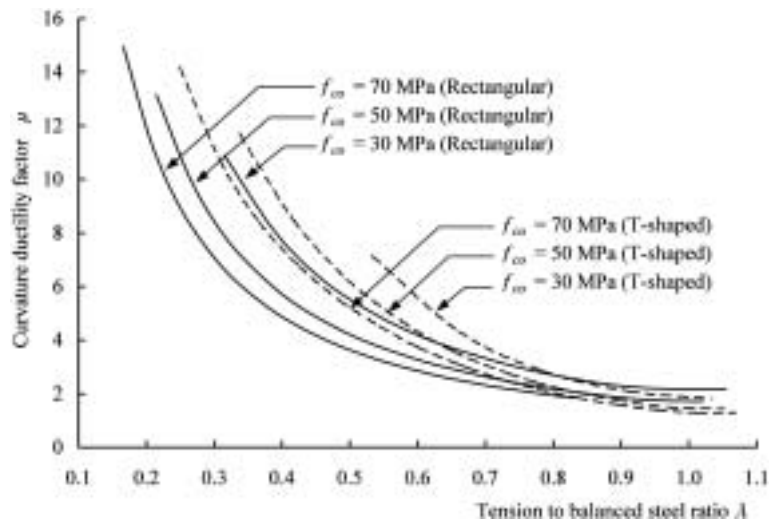


Fig. 8 Variation of curvature ductility factor μ with tension to balanced steel ratio λ

steel ratio (i.e., the same degree of the beam section being under/over-reinforced), the flexural ductility of the beam section decreases as the concrete grade increases. This is in line with the fact that a higher grade concrete is generally less ductile. Nevertheless, the concrete grade has only secondary effect on flexural ductility. The effect of the tension to balanced steel ratio far outweighs the effect of the concrete grade and that is why at a fixed tension steel area, the flexural ductility actually increases with the concrete grade.

5. Effect of sectional shape on flexural ductility

5.1. Parametric study

In order to study the effect of sectional shape on flexural ductility, a number of beam sections with different B_w/B and D_f/D ratios have been analysed by using the method developed herein. All together, 16 T-shaped sections with B_w/B and D_f/D ratios ranging from 0.1 to 0.4 and one rectangular section with the same overall dimensions have been analysed. The 16 T-shaped sections are numbered from T-1 to T-16 while the rectangular section is named as RECT, as listed in Table 1. All the beam sections analysed have overall dimensions of $B=1000$ mm and $D=1500$ mm. For each beam section, the concrete strength f_{co} is set equal to 30, 50 or 70 MPa and the tension to

Table 1 Beam sections analysed in the parametric study

B_w/B	D_f/D				
	0.1	0.2	0.3	0.4	1.0
0.1	T-1	T-2	T-3	T-4	-
0.2	T-5	T-6	T-7	T-8	-
0.3	T-9	T-10	T-11	T-12	-
0.4	T-13	T-14	T-15	T-16	-
1.0	-	-	-	-	RECT

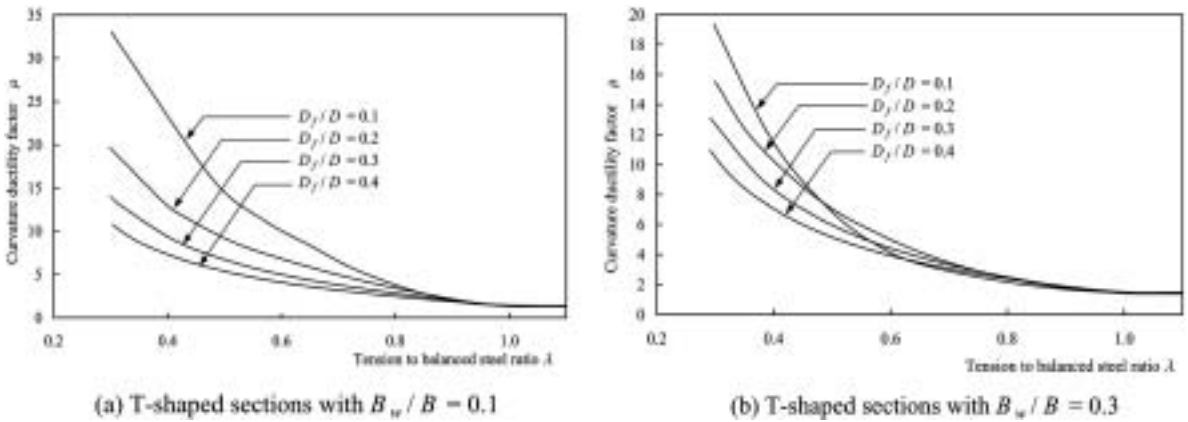


Fig. 9 Effect of flange depth on flexural ductility

balanced steel ratio λ is varied from 0.1 to 1.2. However, to reduce the number of variables, the tension steel yield strength f_{yt} is fixed at 460 MPa.

5.2. Effect of flange depth

To illustrate the effect of flange depth, the μ -values of T-shaped sections with D_f/D ratios ranging from 0.1 to 0.4 and B_w/B ratios set equal to a fixed value are plotted against the corresponding λ -values in Fig. 9. From the curves plotted in Fig. 9(a) and Fig. 9(b) for sections with $B_w/B=0.1$ and 0.3 respectively, it can be seen that the effect of the D_f/D ratio on the flexural ductility is dependent on the value of λ . Basically, when λ is small, a smaller flange depth or D_f/D ratio would lead to a higher flexural ductility. However, it should be noted that a smaller flange depth would lead to a smaller balanced steel area and, for a given tension steel area, a higher value of λ . Hence, at the same tension steel area, a smaller flange depth would still result in a lower flexural ductility.

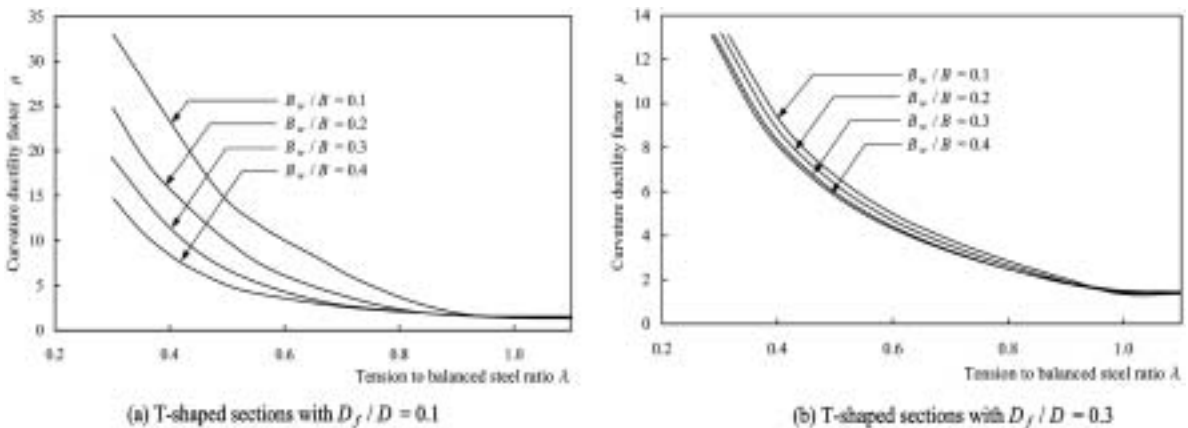


Fig. 10 Effect of web breadth on flexural ductility

5.3. Effect of web breadth

To illustrate the effect of web breadth, the μ -values of T-shaped sections with B_w/B ratios ranging from 0.1 to 0.4 and D_f/D ratios set equal to a fixed value are plotted against the corresponding λ -values in Fig. 10. From the curves plotted in Fig. 10(a) and Fig. 10(b) for sections with $D_f/D=0.1$ and 0.3 respectively, it can be seen that the B_w/B ratio has relatively larger effect on the flexural ductility when D_f/D is small, especially if at the same time the value of λ is small. In general, when λ is small, a smaller web breadth or B_w/B ratio would lead to a higher flexural ductility. However, it should also be noted that a smaller web breadth would lead to a smaller balanced steel area and, for a given tension steel area, a higher value of λ . Hence, at the same tension steel area, a smaller web breadth would still result in a lower flexural ductility.

5.4. Minimum ductility design of non-rectangular beams

To ensure the provision of a certain minimum level of flexural ductility, it is a common practice to set a maximum limit to the tension steel ratio of the beam section to be designed. In the American Code ACI 318, the tension steel ratio is limited to be not more than 0.75 of the balanced steel ratio, while in the British Standard BS 8110, the tension steel ratio is limited to be not more than that leading to a neutral axis depth equal to 0.5 of the effective depth. These two codes have been in use for a long time and presumably are applicable mainly to normal concrete beams rather than high-strength concrete beams. It has been shown that for beams cast of normal concrete with $f_{co}=30$ MPa, ACI 318 would yield a minimum curvature ductility factor μ of 3.32 whereas BS 8110 would yield a minimum curvature ductility factor μ of 3.22 (Ho, *et al.* 2004). Herein, it is suggested to impose the minimum curvature ductility factor to be achieved for all beams, including rectangular and non-rectangular, normal and high-strength concrete beams, as 3.32 in order to

Table 2 Maximum tension to balanced steel ratios for $\mu \geq 3.32$ ($f_{co}=30$ MPa)

B_w/B	D_f/D				
	0.1	0.2	0.3	0.4	1.0
0.1	0.81	0.79	0.77	0.75	-
0.2	0.79	0.77	0.75	0.73	-
0.3	0.77	0.75	0.74	0.72	-
0.4	0.75	0.73	0.72	0.72	-
1.0	-	-	-	-	0.75

Table 3 Maximum tension to balanced steel ratios for $\mu \geq 3.32$ ($f_{co} = 50$ MPa)

B_w/B	D_f/D				
	0.1	0.2	0.3	0.4	1.0
0.1	0.75	0.72	0.69	0.66	-
0.2	0.72	0.69	0.66	0.64	-
0.3	0.69	0.66	0.64	0.62	-
0.4	0.65	0.63	0.62	0.61	-
1.0	-	-	-	-	0.62

Table 4 Maximum tension to balanced steel ratios for $\mu \geq 3.32$ ($f_{co} = 70$ MPa)

B_w/B	D_f/D				
	0.1	0.2	0.3	0.4	1.0
0.1	0.72	0.68	0.64	0.60	-
0.2	0.68	0.65	0.61	0.58	-
0.3	0.64	0.61	0.58	0.56	-
0.4	0.60	0.58	0.56	0.54	-
1.0	-	-	-	-	0.55

maintain a consistent minimum level of flexural ductility.

It is considered that the best way to ensure the achievement of the above required minimum curvature ductility factor is to set a maximum limit to the tension to balanced steel ratio λ . From the parametric study, the maximum values of λ that would lead to a minimum value of $\mu=3.32$ for beam sections with different shapes and cast of different grades of concrete have been evaluated, as presented in Tables 2, 3 and 4. These maximum values of λ can be used directly for the minimum ductility design of non-rectangular concrete beams.

It is evident from the results presented in the tables that at the same concrete strength, the maximum value of λ does vary with the B_w/B and D_f/D ratios. Nevertheless, in most cases, the maximum value of λ for a non-rectangular beam is somewhat larger than that for a rectangular beam. It is only when $B_w/B \approx 0.4$ and $D_f/D \approx 0.4$ would the maximum value of λ become slightly smaller than that for a rectangular beam. Hence, for simplicity, in the design of a non-rectangular beam, provided the balanced steel ratio is evaluated with the sectional shape taken into account, the non-rectangular beam may be deemed to have satisfied the minimum flexural ductility requirement if its tension to balanced steel ratio is not higher than the maximum allowable value of tension to balanced steel ratio for a rectangular beam cast of the same concrete.

6. Conclusions

The nonlinear flexural analysis method previously developed by the authors' team has been improved by changing from trapezoidal to Romberg integration and from the use of extrapolation in the iterations to the use of interpolation to increase its numerical accuracy and stability. Using this improved analysis method, the post-peak flexural behaviour of non-rectangular beams of various shapes has been analysed. From the analytical results, the following conclusions may be drawn:

- (1) At the same tension steel area, the flexural ductility of a T-, Γ -, Π - or box-shaped section is lower than that of a rectangular section with the same overall dimensions.
- (2) At the same tension to balanced steel ratio, the flexural ductility of a T-, Γ -, Π - or box-shaped section is slightly higher than that of the rectangular section when the sections are lightly reinforced and slightly lower than that of the rectangular section when the sections are heavily reinforced.
- (3) The main effect of changing from a rectangular section to a T-, Γ -, Π - or box-shaped section is the significant reduction of the balanced steel area of the beam section. That is why at a given tension steel area, a T-, Γ -, Π - or box-shaped section would have a higher tension to balanced steel ratio and thus a lower flexural ductility.

A parametric study on the effect of sectional shape on the flexural ductility of non-rectangular, normal and high-strength concrete beams has been carried out. Based on the results of the parametric study, the maximum allowable values of tension to balanced steel ratio that would ensure the provision of a minimum curvature ductility factor of 3.32 have been evaluated. These maximum allowable values of tension to balanced steel ratio can be used directly for the minimum ductility design of non-rectangular, normal and high-strength concrete beams. Nevertheless, for simplicity, since the maximum allowable value of tension to balanced steel ratio for a non-rectangular beam is in most cases larger than that for a rectangular beam, a non-rectangular beam may be deemed to have satisfied the minimum flexural ductility requirement if its tension to balanced steel ratio is not higher than the maximum allowable value for a rectangular beam cast of the same concrete.

Acknowledgements

The work described in this paper was carried out with financial support provided by the Croucher Foundation of Hong Kong.

References

- Attard, M. M. and Setunge, S. (1996), "The stress strain relationship of confined and unconfined concrete", *ACI Materials*, **93**(5), 432-444.
- Carreira, D. J. and Chu, K. H. (1986), "The moment-curvature relationship of reinforced concrete members", *ACI*, **83**(2), 191-198.
- Gerald, C. F. and Wheatley, P. O. (1999), *Applied Numerical Analysis*, 6th Ed., Addison-Wesley, USA, 698pp.
- Ho, J. C. M., Kwan, A. K. H. and Pam, H. J. (2003), "Theoretical analysis of post-peak flexural behavior of normal- and high-strength concrete beams", *Structural Design of Tall and Special Buildings*, **12**, 109-125.
- Ho, J. C. M., Kwan, A. K. H. and Pam, H. J. (2004), "Minimum flexural ductility design of high-strength concrete beams", *Magazine of Concrete Research*, **56**(1), 13-22.
- Kwan, A. K. H., Ho, J. C. M. and Pam, H. J. (2002), "Flexural strength and ductility of reinforced concrete beams", *Proc., Institution of Civil Engineers, Structures and Buildings*, **152**(4), 361-369.
- Kwan, A. K. H., Ho, J. C. M. and Pam, H. J. (2004), "Effects of concrete grade and steel yield strength on flexural ductility of reinforced concrete beams", *Australian Journal of Structural Engineering*, **5**(2), 119-138.
- Pam, H. J., Kwan, A. K. H. and Islam, M. S. (2001a), "Flexural strength and ductility of reinforced normal- and high-strength concrete beams", *Proc., Institution of Civil Engineers, Structures and Buildings*, **146**(4), 381-389.
- Pam, H. J., Kwan, A. K. H. and Ho, J. C. M. (2001b), "Post-peak behavior and flexural ductility of doubly reinforced normal- and high-strength concrete beams", *Struct. Eng. Mech., An int. J.*, **12**(5), 459-474.
- Park, R. and Paulay, T. (1975), *Reinforced Concrete Structures*; John Wiley & Sons, New York, USA, 769pp.
- Samra, R. M., Deeb, N. A. A. and Madi, U. R. (1996), "Transverse steel content in spiral concrete columns subjected to eccentric loading", *ACI Struct.*, **93**(4), 412-419.
- Skeikh, S.A. and Yeh, C. C. (1992), "Analytical moment-curvature relations for tied concrete columns", *Struct. Eng., ASCE*, **118**(2), 529-544.

Notation

- A_{sc} , A_{st} = areas of compression and tension steel reinforcement respectively
 $A_{st,bo}$ = balanced steel area
 B = breadth of beam section
 B_w = breadth of the web or total breadth of the webs

b	=breadth at x from neutral axis
D	=effective depth of beam section
D_f	=depth of compression flange
D_1	=depth of compression reinforcement
d_n	=depth of neutral axis
E_s	=Young's modulus of steel reinforcement
f_{co}	=in-situ uniaxial compressive strength of concrete
f_{yt}	=yield strength of tension steel reinforcement
M	=moment acting on beam section
M_p	=peak resisting moment of beam section
P	=axial load acting on beam section
R	=unbalanced axial force acting on beam section
x	=distance from neutral axis
ε	=strain in beam section
ε_c	=strain in concrete
ε_{ce}	=strain at the extreme concrete compression fibre
ε_{co}	=strain in concrete at peak stress
$\varepsilon_{sc}, \varepsilon_{st}$	=strains in compression and tension reinforcement respectively
ϕ	=curvature of beam section
ϕ_u, ϕ_y	=ultimate and yield curvatures of beam section respectively
λ	=degree of beam section being under/over-reinforced
μ	=curvature ductility factor
σ_c	=stress developed in concrete
σ_{sc}, σ_{st}	=stresses developed in compression and tension reinforcement respectively
CC	